10.24425/acs.2022.140866

Archives of Control Sciences
Volume 32(LXVIII), 2022
No. 1, *pages* 85–103

Observer design estimating the propofol concentration in PKPD model with feedback control of anesthesia administration

Muhammad ILYAS, Awais KHAN, Muhammad Abbas KHAN, Wei XIE, Raja Ali RIAZ and Yousaf KHAN

Propofol infusion in anesthesia administration requires continual adjustment in the manual infusion system to regulate the hypnosis level. Hypnotic level is based on Bispectral Index Monitor (BIS) showing the cortical activity of the brain scaled between 0 to 100. The new challenging aspect of automation in anaesthesia is to estimate the concentration of hypnotic drugs in different compartments of the body including primary, rapid peripheral (muscle), slow peripheral (bones, fat) and effect site (brain) compartment based on Pharmacokinetics (PK) and Pharmacodynamics (PD) model. This paper aimed to regulate the hypnosis level with estimating the Propofol concentrations using a linear observer in feedback control strategy based on Integral Super-Twisting Sliding Mode Controller (ISTSMC). The drug concentration in plasma of the silico patients accurately estimated in nominal transient. The results show that tracking errors between the actual output in form of BIS level and linearized output nearly approaches to zero in the maintenance phase of anesthesia to ensure the controller response on sliding phase with optimum performances by achieving desired hypnotic level 50 on BIS. The robustness of

Muhammad Ilyas (e-mail: m.ilyas@buetk.edu.pk) is with the Department of Electrical Engineering, Balochistan University of Engineering and Technology Khuzdar, Pakistan.

Awais Khan (corresponding author, e-mail: awaiskhan@szu.edu.cn) the corresponding author is with the College of Mechatronics and Control Engineering and Key Laboratory of Optoelectronic Devices and Systems of Ministry of Education and Guangdong Province, Shenzhen University, Shenzhen 518060, China.

Muhammad Abbas Khan (e-mail: muhammad.abbas@buitms.edu.pk) is with the Department of Electrical Engineering, Balochistan University of Information Technology, Engineering and Management Sciences, Quetta, Pakistan.

Wei Xie (e-mail: weixie@scut.edu.cn) is with College of Automation Science and Technology, South China University of Technology, Guangzhou 510641, People's Republic of China.

Raja Ali Riaz (e-mail: rajaali@comsats.edu.pk) is with the Department of Electrical and Computer Engineering, Comsats University Islamabad 45550, Pakistan.

Yousaf Khan (e-mail: yousafkhalil@gmail.com) is with Department of Electrical Engineering, Univeristy of Engineering and Technology Peshawar, Peshawar, Pakistan.

This work was supported in part by Key-Area Research and Development Program of Foshan City under Grant 2020001006812.

Received 28.08.2021. Revised 1.03.2022.

control strategy is further ensured by adding measurement noise of electromagnetic environment of operation theatre distracting signal quality index of the output BIS level.

Key words: pharmacokinetic and pharmacodynamic models, bispectral index monitor, observer design, sliding mode control

1. Introduction

Advancement in control engineering diverts the manual drug delivery system concepts in clinical surgery. The surgical procedure can be carried out with little effort in the current era. Such advancement is possible with research outcomes in health care engineering. Initially, the surgical procedure needs fast execution due to lack of anaesthetics and applied different schemes like application of cold, nerve's compression to keep the patient unconscious [1]. In 1840, Hickman invented the inhalation gases, which enabled invasive surgeries. C.W. Long, in 1842, used diethyl-ether to conduct surgical procedures that extend to term anesthesia, meaning lack of sense [2]. Anesthetic drug infusion based on three significant ingredients, including hypnotic, analgesic and areflexia, aimed to ensure lack of sense, pain and movements, respectively. Moreover, anesthesia administration consists of three main phases: induction, maintenance and emergence [3]. In the transient phase hypnotic drugs are being administered to the patient to achieve the desired unconscious level. The second phase is the maintenance phase to conduct the surgical procedure with optimum delivery of drug infusion. As the surgical procedure is completed, it directs to the emergence phase to stop the drug infusion and skin closure procedure is initialized to bring the patients to consciousness. The general surgery is performed during the maintenance phase of anesthesia with hypnosis level between 40 and 60 on BIS [4–8].

Using general anesthesia propofol as hypnotic agent and fast acting opioids, e.g. remifentanil is used as a pain killer. Both of these drugs have synergistic effects on patients [9]. There are two main issues in manual drug delivery of anesthesia, under-dosing and over-dosing of anesthetics. Under-dosing of anesthetics causes awareness, which leads to vomiting and anxiety, and over-dosing of anesthesia leads to cardiovascular collapse. Both of these states are unacceptable to clinical professionals during surgery [10]. Careful management of drug induction is the crucial factor in the successful conduction of surgical procedures. All these limitations in manual drug delivery of anesthetics reflect the attention of the scientific community to realize automation in anesthesia.

Targeted Controlled Infusion (TCI) is a computer-assisted open loop drug delivery system that administers the required anaesthetics level without considering the feedback signal. Such a system is based on population-based pharmacokinetic and pharmacodynamic modeling. PK model shows the rate of metabolism

of drugs within the human body and the PD model identifies the drugs on the brain side referred to as an effect-site compartment. The effect of hypnotic drugs is modeled through a nonlinear sigmoid model indicating the hypnosis level on BIS is scaled between 100 fully awake states and 0 dead states. The general surgery is performed between 40 and 60 on BIS [11, 12].

A closed-loop control system offers several advantages compared to TCI systems, including automatic regulation of hypnosis level and drug infusion rate by reducing the inter-patient and intra-patient variability and eliminating the anesthesiologist intervention [12–14]. Primarily the closed-loop control of anesthesia was introduced by Chao Dong in his doctoral study in 2003 [15]. C. Dong derived a three compartmental PK-PD model for hypothetical patients and linearized it using linear regression. The limitation of Dong work due to significant variation in hypnosis level during maintenance phase beyond the acceptable level [15]. Soltesz et al., worked on the same phenomena to regulate the hypnosis level on BIS using propofol and remifentanil as hypnotic and analgesic components of anesthesia, respectively.

The major significance of his work is revealed in his doctoral research work due to practical experiments to be carried out on 47 validated models attaining the interpatient variability. The controller applied was based on multi-inputs, including propofol and remifentanil [16–19]. Soltesz et., did not focus on handling the intra-patient variability like blood pressure variation, bleeding, which can affect the smooth conduction of surgery. Moreover, the control engineering community has not addressed measuring the concentration of drugs in different compartments of the body based on the PK-PD model due to the lack of such a sensor.

The corresponding research work is based on observer design in a closed-loop fashion with a ISTSMC to estimate the non measurable states in the form of drug concentration in different body compartments. The drug concentration in different compartments, including primary, rapid peripheral, slow peripheral and effect-site compartments, are estimated based on Luenberger observer. The feedback controller is designed using estimated states of the observer-based on ISTSMC. The ISTSMC is applied due to fast transient response and minimal steady state error and immune to measurement noise added to output BIS level that occurs due interference signal of electromagnetic environment of operation theatre distracting the signal quality index of electrode of BIS monitor fixed on forehead of the patient.

The rest of the paper is organized as follows. Section 2 explains the three compartment PK-PD model. Section 3 focuses on observer design to simulate the controllability and observability of the proposed system whereas Section 4 consists of controller design. The results are explained and discussed in Section 5. Finally, Section 6 comments on conclusion.

2. Pharmacokinetic and pharmacodynamic modeling

The dynamics of infusion drugs in the patient body is classified into PK-PD model [20–22]. The PK model shows how the drug is metabolized within the human blood plasma [22]. The PD model exhibits the drug concentration at the effect site like the brain [23–25]. The blood within the human body acts as a carrier to transmit the drug to different body organs. The overall human body is categorized into different compartments based on the drug flow rate, including primary, rapid peripheral and slow peripheral compartments [1]. The primary compartment (intravascular blood) with volume V_1 is shown in the centre of Figure 1. Moreover, the muscles are represented by rapid peripheral compartment V_2 and fates are represented by slow peripheral compartment V_3. Both of these compartments are connected to the primary compartment through weighted rate constants k_{12}, k_{21}, k_{13} and k_{31}. The flow of anesthetic agents amongst different compartments occurred exponentially [4]. The drug's overall effect is measured on the brain in terms of cortical activity measured on BIS scaled between 100 to 0.

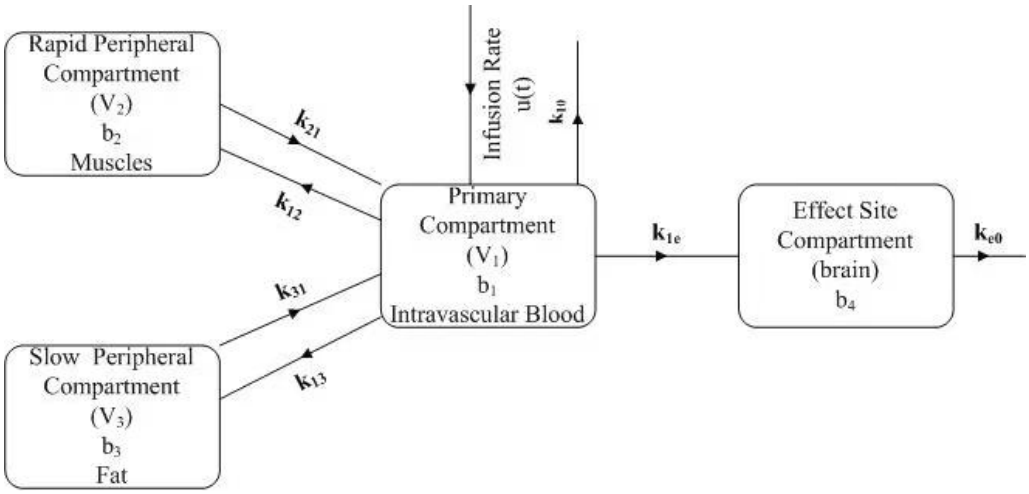

Figure 1: Block diagram of PK and PD models

The state equations for three compartmental model with additional effect site compartment is described in equations (1)–(4) in [23–25] as:

$$\dot{b_1}(t) = -k_{10}b_1(t) - k_{12}b_1(t) - k_{13}b_1(t) + k_{21}b_2(t) + k_{31}b_3(t) + u(t), \quad (1)$$

$$\dot{b_2}(t) = k_{12}b_1(t) - k_{21}b_2(t), \quad (2)$$

$$\dot{b_3}(t) = k_{13}b_1(t) - k_{31}b_3(t). \quad (3)$$

PD model presents the drug concentration at the effect site (brain) given in equation (4) as:

$$\dot{b_4}(t) = k_{1e}b_1(t) - k_{e0}b_4(t). \tag{4}$$

The b_1, b_2, b_3 and b_4 that mentioned in equations (1)–(4) indicate the drug concentration in primary, rapid peripheral, slow peripheral and effect site compartment respectively measured in mg and u shows the drug infusion through ISTSMC measured in mg/sec.

The output of infusion drug based on their effect at brain site mapped through nonlinear sigmoid model is shown in equation (5) as:

$$BIS(t) = E_0 - E_{\max} \times \frac{{b_4}^{\gamma}}{b_4 + {C_{50}}^{\gamma}}. \tag{5}$$

In above stated Eq. (5) E_0 indicates the fully awake state of the silico patient, $E_{\max}$ shows the maximum effect achieved using hypnotic agent, C_{50} shows the half of the maximum effect and γ shows the slope of the sigmoid curve.

The clinical parameters using patient attributes based Schneider PK-PD model [24, 25] including the Lean Body Mass(LBM) of male is $1.1 \cdot W - 128W^2/H^2$ and LBM of female is $1.07 \cdot W - 148W^2/H^2$. Similarly the weighted rated constant k_{10}, k_{13}, k_{21} and k_{31} are C_{l1}/V_1, C_{l3}/V_1, C_{l2}/V_2 and C_{l3}/V_3 respectively. The volume of the compartment is V_1, V_2 and V_3 is $4.27[l]$, $18.9 - 0.391(Age-53)[l]$ and $238[l]$ respectively. The clearance (Cl) predicts the ability of the body to nullify and remove the effect of the drugs by elimination through kidneys. The clearance of different compartments in PK-PD model including C_{l1}, C_{l2} and C_{l3} is $1.89 + 0.0456(W - 77)$-$0.0681(LBM - 59)$+$0.0264(H - 177)$, 1.29-$0.024(Age - 53)$ and 0.836, respectively.

3. Observer design

The core objective of observer design is the state estimation of three compartmental PK-PD models that predict the drug concentration in the plasma of different compartments of the body [26]. As it is evident from literature that there is no biomedical sensor to predict and measure the plasma drug concentration after infusion of anesthetic agents to the human body. Equations (6) and (7) show the state space representation of the PK-PD model. The output of the PK-PD is non linear sigmoid model mentioned in equation (5) is linearized through optimal linearization method. As the C matrix is changed and $(A - LC)$ becomes negative definite through scheduling the gain L of the observer.

$$\dot{b} = Ab + Bu, \tag{6}$$

$$y = Cb, \tag{7}$$

where b is the states of PK-PD model, A is the input state matrix, C is the output state matrix. The estimated states of the observer are given as:

$$\dot{\hat{b}} = A\hat{b} + Bu + L(y - C\hat{b}), \tag{8}$$

$$y = C\hat{b}. \tag{9}$$

The above mathematical expression in equations (8), (9) shows the luenberger observer with $A\hat{b}+Bu$ is the replica of the plant dynamics and $L(y-C\hat{b})$ estimate the future states based on current estimation error. The L shows the gain scheduled and tuned iteratively. The equation (8) can be simplify as:

$$\dot{\hat{b}} = \hat{b}(A - LC) + Bu + Ly. \tag{10}$$

The error function (E) are defined as:

$$E = b - \hat{b}. \tag{11}$$

By taking derivative of the above error function (E) as:

$$\dot{E} = \dot{b} - \dot{\hat{b}}\,. \tag{12}$$

Putting the value of $\hat{b}$ and $\dot{\hat{b}}$ in error function in equation (12),

$$\dot{E} = Ab + Bu - \left(A\hat{b} + Bu + L(y - C\hat{b})\right), \tag{13}$$

$$\dot{E} = \left(b - \hat{b}\right)(A - LC). \tag{14}$$

3.1. Observer error (E) convergence matrix

The gain L of the observer is tuned using gain scheduling algorithems as that matrix $(A - LC)$ has eigenvalues (λ) with negative values. The matrix $(A - LC) < 0$ will be negative definite as:

$$A = \begin{pmatrix} -k_{10} - k_{12} - k_{13} & k_{21} & k_{31} & 0 \\ -k_{12} & -k_{21} & 0 & 0 \\ k_{13} & 0 & -k_{31} & 0 \\ k_{1e} & 0 & 0 & -k_{e0} \end{pmatrix}, \tag{15}$$

$$B = \begin{pmatrix} 1 & 0 & 0 & 0 \end{pmatrix}. \tag{16}$$

The output equation for the PK-PD model as defined in equation (5) linearized through optimal linearization and matrix C is changed as by tuning the gain L such as the $(A - LC)$ becomes negative definite.

3.2. Simulation and results of observer design

Figure 2 shows the observability and controllability of the state matrix is full rank as the order of the system is 4×4. Before controller design it is quite important the check the observability and controllability of the state matrix that either the proposed system is full rank or not. In this case Figure 2 shows that state matrix is full rank.

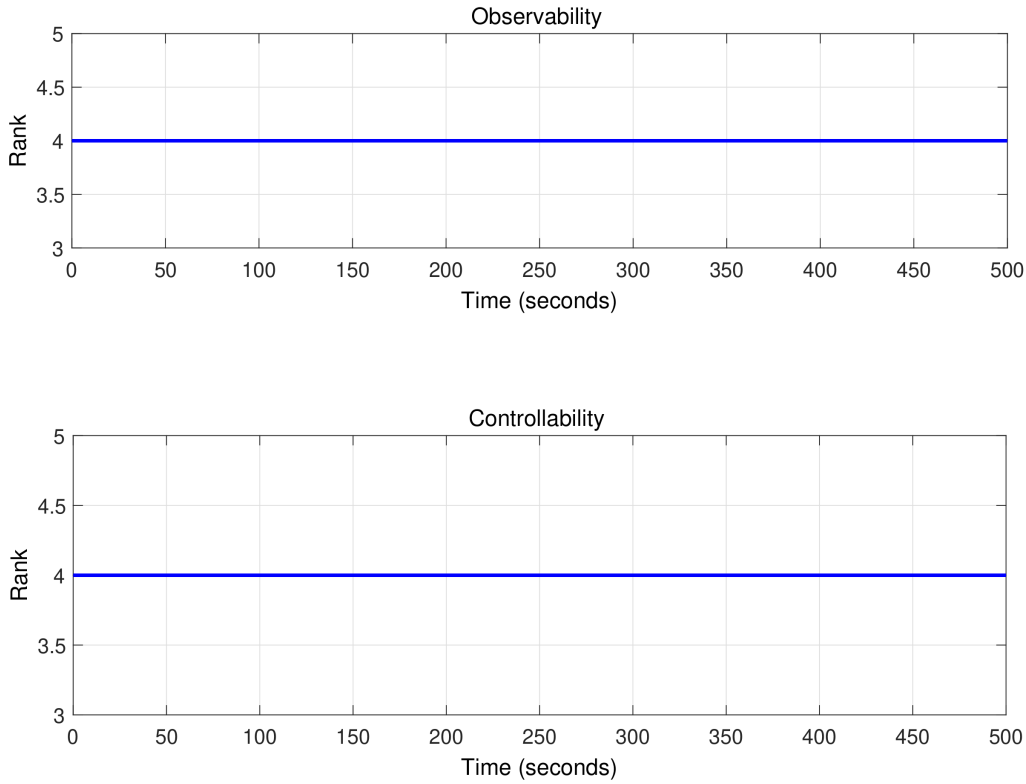

Figure 2: Rank of observability and controllability matrix

Figure 3 shows the eigenvalues of the error convergence matrix. All four eigenvalues (λ) decay from zero to negative values along the axis. It predicts that is negative definite of the state matrix of PK-PD model.

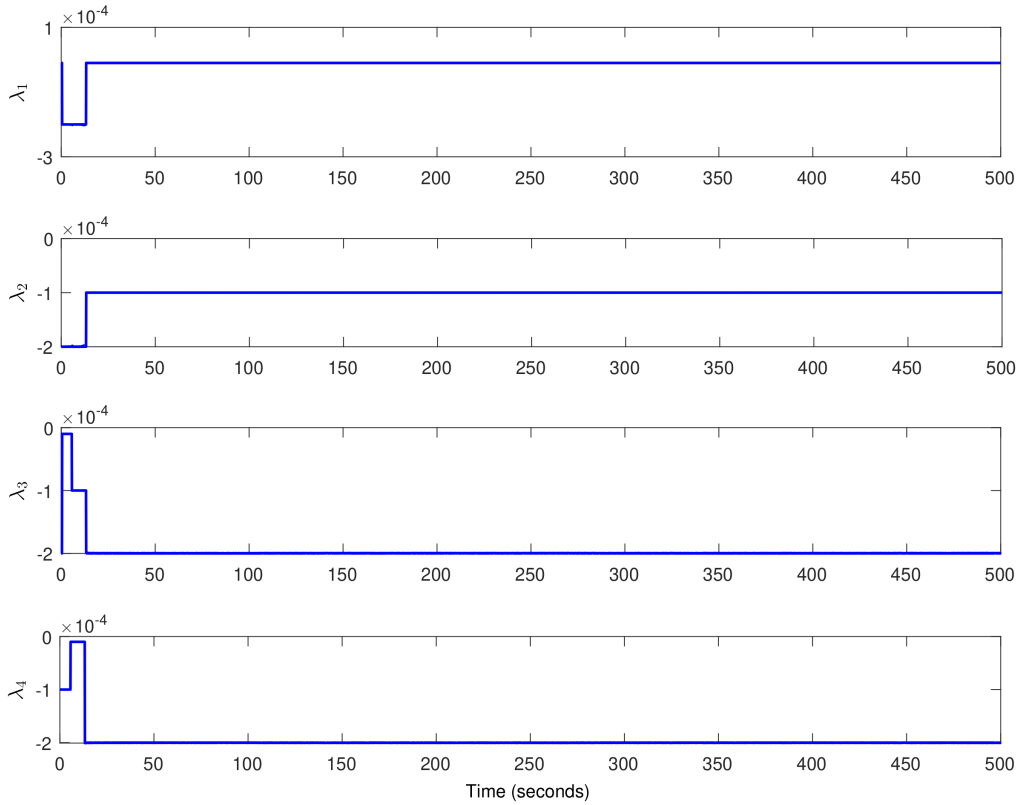

Figure 3: Eigenvalues of error convergence matrix

4. Integral super-twisting sliding mode control (ISTSMC) design

The nonlinear ISTSMC is based on a nonlinear sliding surface showing robustness to the external disturbances including measurement noise, electrical signal interference from electrical equipment in the operation theatre. The primary significance of ISTSMC showing rapid transient response and less steady-state error in the presence of disturbances [27–29].

The sliding manifold chosen as to achieve the required performance as:

$$\sigma = \dot{e} + (\lambda_1)e + (\lambda_2)\int (e)\,\mathrm{d}t, \tag{17}$$

$$e = BIS_{\mathrm{des}} - BIS_{\mathrm{act}}\,, \tag{18}$$

where $BIS_{\mathrm{des}} = 50$ is the desired hypnotic level on BIS required for conduction surgical procedure and and $\lambda_1 \in \Re^+$ is a design parameter. Ideally the sliding

manifold shall be ($\sigma = 0$) can be expressed as:

$$\sigma = \dot{e} + (\lambda_1)e + (\lambda_2)\int (e)\,\mathrm{d}t = 0. \tag{19}$$

By simplifying the equation (19) as $e(t)$ asymptotically converges to zero as:

$$e(t) = e(0)te^{-\lambda_1 t}. \tag{20}$$

The equation (20) predicts that error function $e(t)$ shall be decaying exponentially as $t > 0$. The control law is designed by taking the derivative of equation (19) as:

$$\dot{\sigma} = \ddot{e} + (\lambda_1)\dot{e} + (\lambda_2)e, \tag{21}$$

$$\dot{e} = 0 - E_{\max} \times \frac{\mathrm{d}}{\mathrm{d}t}\left(\frac{b_4(t)^{\gamma}}{b_4(t) + {C_{50}}^{\gamma}}\right), \tag{22}$$

$$\ddot{e} = \frac{E_{\max}{b_4}^{\gamma}\ddot{b_4}}{(K + b_4)^2} - \frac{2 \times E_{\max}{b_4}^{\gamma}\dot{b_4}^2}{(K + b_4)^3} + \frac{2 \times E_{\text{peak}}\gamma{b_4}^{\gamma-1}\dot{b_4}^2}{(K + b_4)^2} - \frac{E_{\max}\gamma{b_4}^{\gamma-1}\ddot{b_4}}{K + b_4} - (\gamma - 1) \times \frac{E_{\max}\gamma{b_4}^{\gamma-2}\dot{b_4}^2}{K + b_4}, \tag{23}$$

where $K = C_{50}^{\gamma}$, By putting the value of $\ddot{e}$ from equation (23) and $\dot{e}$ from equation (22) in equation (21), the value of $\dot{\sigma}$ can be realized. To achieve finite time convergence applying reachability law as:

$$\dot{\sigma} = -k_1|\sigma|^{\frac{1}{2}}\mathrm{sign}(\sigma) - k_2\int \mathrm{sign}(\sigma)\,\mathrm{d}\tau, \tag{24}$$

where $k_1, k_2 \in \Re^+$ are controller gain parameters. Now comparing the value of $\dot{\sigma}$ from equation (21) and equation (24) to find the controller input (u) as:

$$-k_1|\sigma|^{\frac{1}{2}}\mathrm{sign}(\sigma) - k_2\int \mathrm{sign}(\sigma)\,\mathrm{d}\tau = \ddot{e} + (\lambda_1)\dot{e} + (\lambda_2)e. \tag{25}$$

By simplifying the equation (25) the controller input (u) derived as:

$$u = \left[\frac{2{\times}E_{\max}{b_4}^{\gamma}\dot{b}_4^2}{(K + b_4)^3} - \frac{2{\times}E_{\max}\gamma{b_4}^{\gamma-1}\dot{b}_4^2}{(K + b_4)^2} + (\gamma{-}1){\times}\frac{E_{\max}\gamma{b_4}^{\gamma-2}\dot{b}_4^2}{K + b_4} - \lambda_1\dot{e} - \lambda_2 e\right] \times \frac{b_4(K + b_4)^2}{E_{\max}b_4^{\gamma}(b_4(1 - \gamma) - K\gamma)(-0.456\dot{b}_4 + 0.1068)} + \left((k_{10} + k_{12} + k_{13})b_1 - k_{21}b_2 - k_{31}b_3\right) - k_1|\sigma|^{\frac{1}{2}}\mathrm{sign}(\sigma) - k_2\int \mathrm{sign}(\sigma)\,\mathrm{d}\tau. \tag{26}$$

5. Results and simulations

Figure 4 shows the closed-loop system with ISTSMC and PK-PD model in cascaded form and nonlinear sigmoid model feedback to observer after linearization. The output from the PK-PD model is mapped on a nonlinear sigmoid model showing the hypnosis level of the patient. The sigmoid model was further linearized using optimal linearization algorithms and applied to Luenberger observer as a feedback signal. The observer estimates the non-measurable states of the patient PK-PD model and adds it to ISTSMC. The core functionality of the controller is to maintain the desired level of hypnosis on BIS by providing a varying level of drug infusion to the patient intravascular blood as a primary compartment.

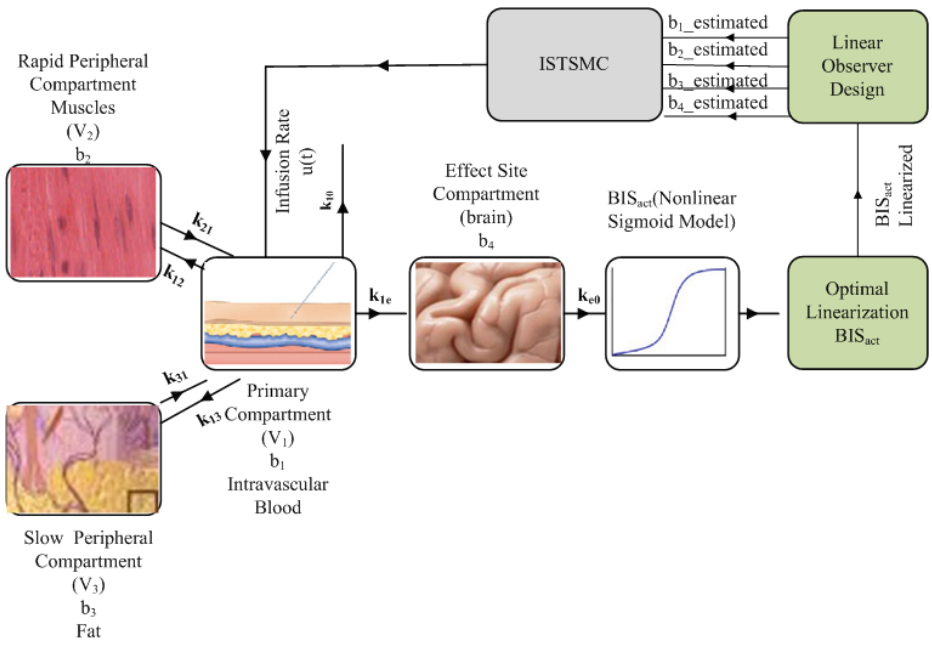

Figure 4: Block diagram of observer design for automatic control of drug infusion in Propofol anesthesia administeration based on ISTSMC

Figure 5 shows the plasma drug concentration in various body compartments, including primary compartment, rapid peripheral compartment, slow peripheral compartment, and effect-site compartment (brain) of actual and estimated states identified by the observer. Initially, the concentration of drug in plasma is maximum in the primary compartment after infusion through intravascular blood and decay exponentially leads to a gradual increase in other compartments of the

body due to distribution and metabolism. The estimated states of the observer shown in Figure 5 accurately track the PK-PD model's actual states.

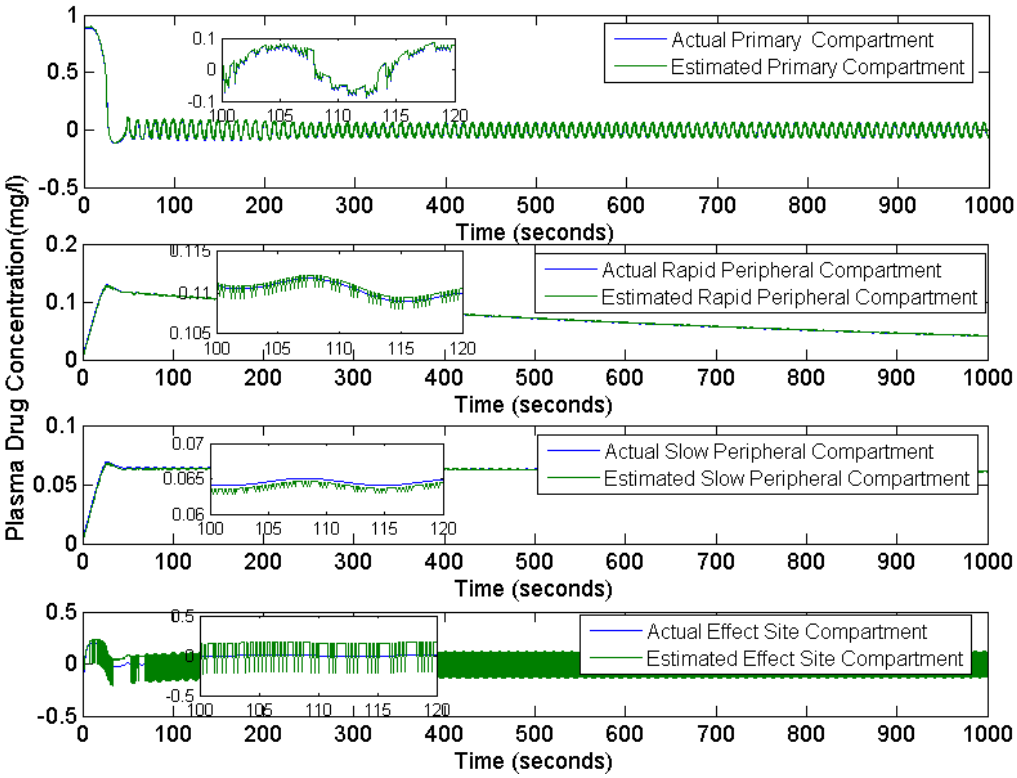

Figure 5: Plasma drug concentration of estimated and actual states of PK-PD model

Figure 6 presents the desired hypnosis level on the BIS monitor for actual, linearized and estimated output. The figure shows that the induction phase is completed achieving the desired hypnotic level 50 in settling time < 70 seconds. A clinical professional initializes the surgical procedure after 70 seconds in the maintenance phase or steady-state phase of anesthesia. The estimated BIS level accurately tracks the actual and linearized output of the system. The steady-state error is initially maximum in the transient phase of drug infusion and reduces significantly to zero nearly in the maintenance phase of anesthesia.

Figure 7 presents the drug infusion level u to the patient body based on ISTSMC applied with estimated state from observer design shown by Figure 4. Figure 7 shows that drug infusion is initially maximum during induction phase of anesthesia to bring the patient from state of consciousness to the hypnotic level. The patient's drug infusion level varies and oscillates to stabilize the hypnosis level on BIS between 40–60.

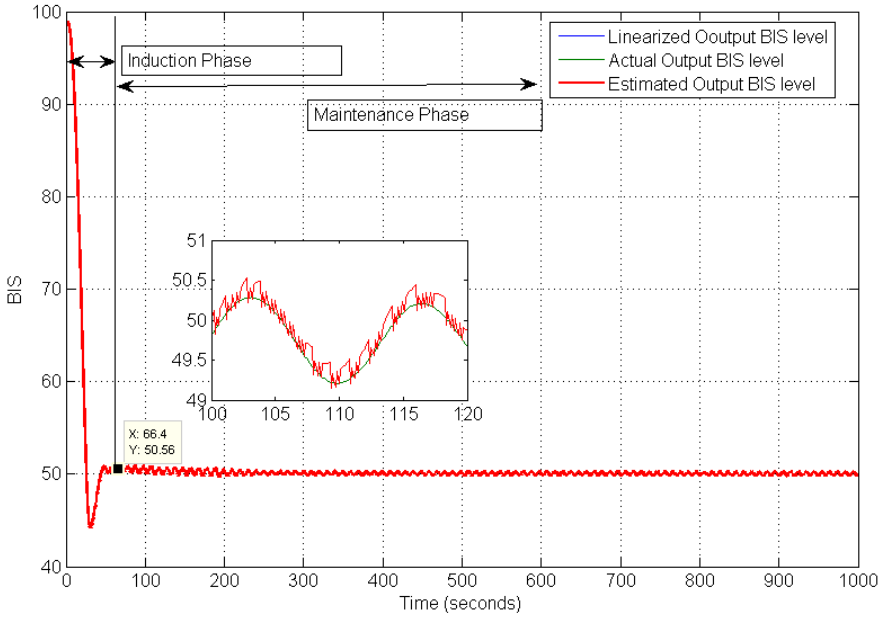

Figure 6: Hynosis level BIS monitor for linearized, estimated and actual output

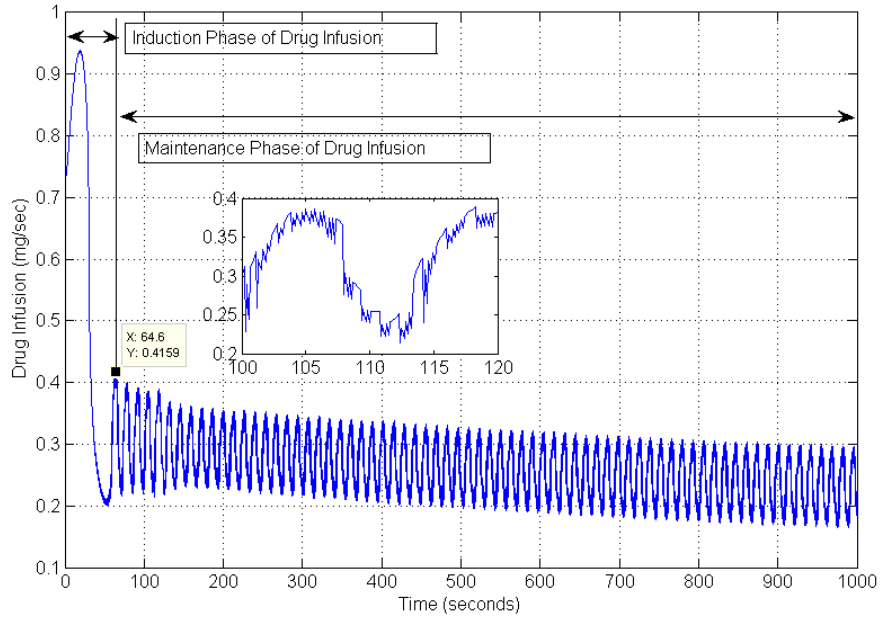

Figure 7: Drug infusion level to the patient based on ISTSMC

5.1. Measurement noise compensation in BIS signal

The BIS monitor extracts the cortical activity of the brain through electrodes placed on the forehead of the patient, as shown in Figure 8. The electrode strip further consists of four electrodes and is fixed on the forehead in major surgery in the supine position [30]. The signal quality index may vary as the position of the electrode varies. Moreover, surgical cautery and other electrical monitoring may interfere with the signal quality index.

Figure 8: Open loop liproscopic surgery conducted in Hayatabad Medical Compplex Peshawar, Pakistan

The measurement noise and interference are also caused by various reasons, including the operation theatre's electromagnetic environment due to multiple equipment working simultaneously that distract the signal quality index of the electrode of the BIS monitor. This paper has added Gaussian noise to the BIS level, as shown in Figure 9. The gaussian has a variance of 0.1 and investigates their effect at controller signal, BIS level, etc.

Figure 10 shows the controller input as a drug infusion based on ISTSMC after adding noise signal due to the electromagnetic environment of the operation theatre. The drug infusion level is maximum during the transient phase or induction phase to bring the patient hypnotic state 40–60 on BIS monitor and then gradually decreases in maintenance phase or steady phase of surgical procedure. The only difference being observed is that the level of chattering slightly increases compared to the controller in figure 7 without considering the noise

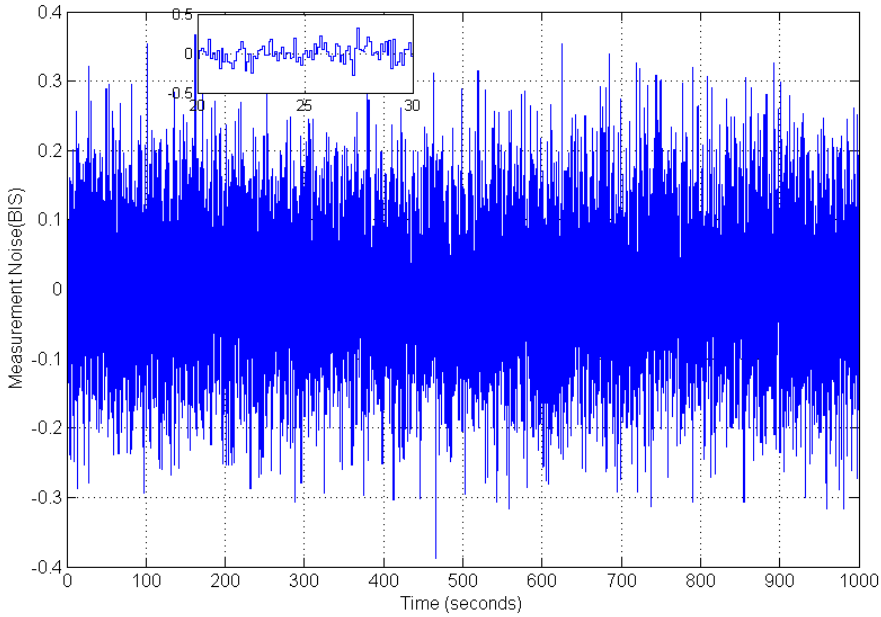

Figure 9: Measurement noise in BIS level

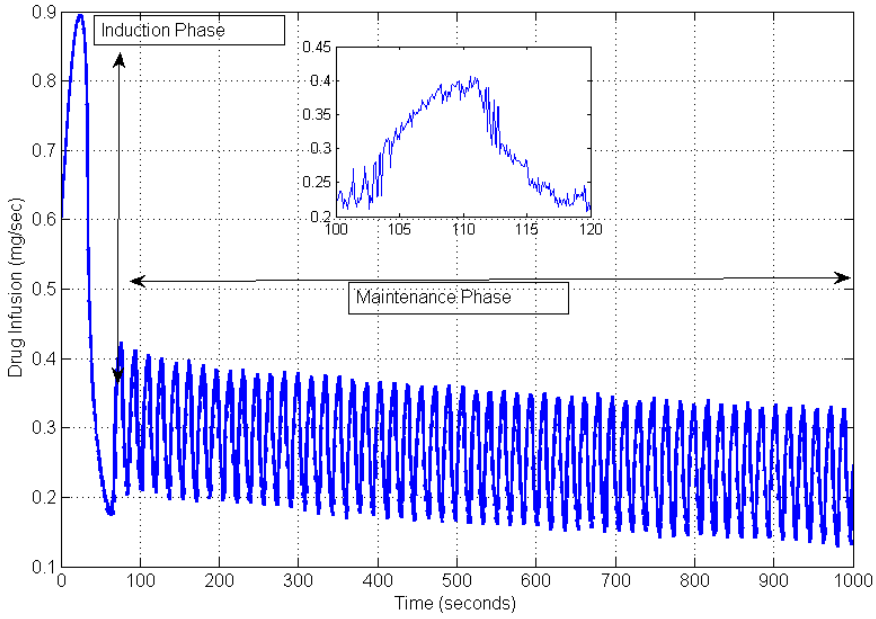

Figure 10: Controller drug infusion after adding the noise signal in the BIS level

and interference. However, the magnitude of the chattering level is tolerable for infusion pumps.

Figure 11 shows the hypnosis level on BIS monitor after considering the noise signal. During the induction phase, undershoot observed slighting exceeding lower limit 40, which is tolerable from clinical view reflecting deep sedation level still ensuring controller robustness to the disturbance and noise signal compensation. The estimated state accurately tracks the actual output and linearized output in anaesthesia administration induction and maintenance. The desired hypnotic level is maintained during the steady-state phase in which surgical procedure is performed.

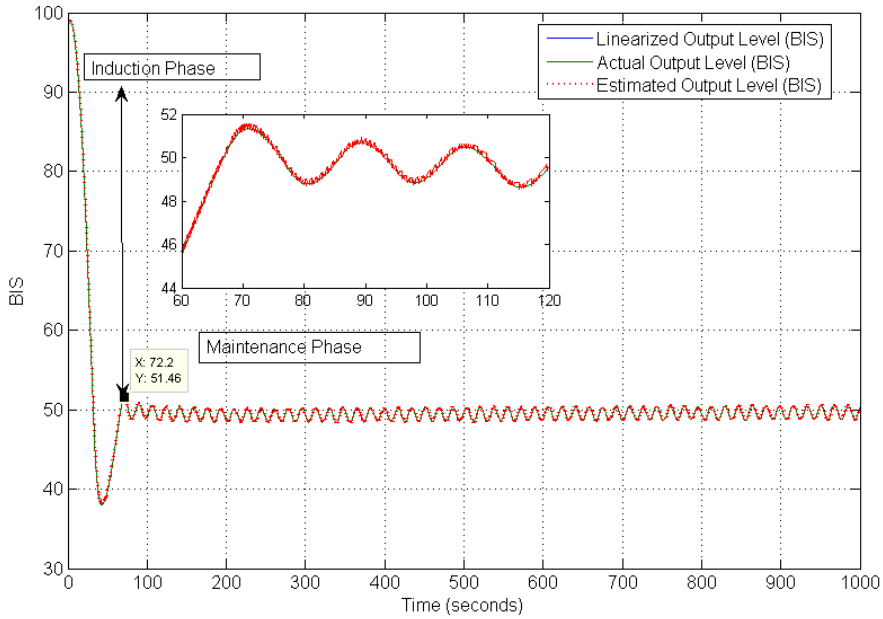

Figure 11: Hynosis level on BIS after adding noise signal

6. Conclusion

This paper proposes observer-based automatic control of drug infusion to regulate the hypnosis level using ISTSMC strategy. The state of the patient PK-PD model consists of plasma drug concentration in different compartments of the body, not measurable parameters with the assistance of any sensor. The linear observer was identified to estimate the actual states of the patient PK-PD model. The ISTSMC administered the optimum level of drug infusion to the patient model to regulate hypnosis levels between 40–60 on BIS. The tracking

error between the actual BIS level as well as linearized and estimated BIS is nearly approaching zero in the maintenance phase of anesthesia. This closed-loop topology of automatic control of drug infusion leads to hardware realization of automation in anesthesia.

References

[1] S. Bibian: Automation in Clinical Anaesthesia. PhD thesis, University of British Columbia, Canada, 2006. DOI: 10.14288/1.0065536.

[2] B.J. Anderson and J. Houghton: Total Intravenous Anesthesia and Target-Controlled Infusion. In *A Practice of Anesthesia for Infants and Children*, 177–198, Elsevier, 2019. DOI: 10.1016/C2015-0-00649-9.

[3] K. Soltesz, K. van Heusden, G.A. Dumont, T. Hagglund, C.L. Petersen, N. West, and J.M. Ansermino: Closed-loop anaesthesia in children using a PID controller: A pilot study. *IFAC Conference on Advances in PID Control*, Brescia, Italy, (2012). DOI: 10.1213/01.ane.0000418552.16222.39.

[4] K. Soltesz, G.A. Dumont, and J.M. Ansermino: Assessing control performance in closed-loop anesthesia. *21st Mediterranean Conference on Control and Automation*, (2013), 191–196. DOI: 10.1109/MED.2013.6608720.

[5] A.A. Spence: The lessons of CEPOD. *British Journal of Anaesthesia*, **60**(7), (1988), 753–754. DOI: 10.1093/bja/60.7.753.

[6] K. van Heusden, J.M. Ansermino, K. Soltesz, S. Khosravi, N. West, and G.A. Dumont: Quantification of the variability in response to propofol administration in children. *IEEE Transactions on Biomedical Engineering*, **60** (2013), 2521–2529. DOI: 10.1109/TBME.2013.2259592.

[7] K. Soltesz, G.A. Dumont, and J.M. Ansermino: Assessing control performance in closed-loop anesthesia. *21st Mediterranean Conference on Control and Automation*, 2013. DOI: 10.1109/MED.2013.6608720.

[8] A.A.V den-Berg, D. Savva, N.M. Honjol, and N.V. Prabhu: Comparison of total intravenous, balanced inhalational and combined intravenous-inhalational anaesthesia for tympanoplasty, septorhinoplasty and adenotonsillectomy. *Anaesth Intensive Care*, **23**(5), (1995) 574–582. DOI: 10.1177/0310057X9502300508.

[9] A.R. Absalom, N. Sutcliffe, and G.N.C. Kenny: Closed-loop control of anaesthesia using Bispectral index: performance assessment in patients undergoing major orthopaedic surgery under combined general and regional anaesthesia. *Anesthesiology*, **96**(1), (2002), 67–73. DOI: 10.1097/00000542-200201000-00017.

[10] K. Soltesz, K. van Heusden, M. Hast, J.M. Ansermino, and G.A. Dumont: A synthesis method for automatic handling of inter-patient variability in closed-loop anesthesia. *American Control Conference*, (2016). DOI: 10.1109/ACC.2016.7526125.

[11] M. Struys, T. De Smet, S. Greenwald, A.R. Absalom, S. Binge, and E.P. Mortier: Performance evaluation of two published closed-loop control systems using bispectral index monitoring: A simulation study. *Anaesthesiology*, **100**(3), (2004), 640–647. DOI: 10.1097/00000542-200403000-00026.

[12] J-Y. Lan, M.F. Abbod, R.G. Yeh, S.Z. Fan, and J.S. Sheih: Review: Intelligent modelling and control in anaesthesia. *Journal of Medical and Biological Engineering*, **32**(5), (2012), 293–307. DOI: 10.5405/jmbe.1014.

[13] D.V. Caiado, J.M. Lemos, and B.A. Costa: Robust control of depth of anesthesia based on *H* infinity design. *Archives of Control Sciences*, **23**(1), (2013), 41–59. DOI: 10.2478/v10170-011-0041-z.

[14] A. Khan, W. Xie, B. Zhang, and L.-W. Liu: A survey of interval observers design methods and implementation for uncertain systems. *Journal of the Franklin Institute*, **358**(6), (2021), 3077–3126. DOI: 10.1016/j.jfranklin.2021.01.041.

[15] C. Dong: Closed Loop Controlled Total Intravenous Anaesthesia. PhD Thesis, University of Plymouth, UK, 2003.

[16] K. Soltesz: On automation in anaesthesia. PhD Thesis, Lund University, Sweden, 2013.

[17] A. Khan, W. Xie, L. Zhang, and Ihsanullah: Interval state estimation for linear time-varying (LTV) discrete-time systems subject to component faults and uncertainties. *Archives of Control Sciences*, **29**(2), (2019), 289–305. DOI: 10.24425/acs.2019.129383.

[18] K. van Heusden, J. M. Ansermino, K. Soltesz, S. Khosravi, N. West, and G.A. Dumont: Quantification of the variability in response to propofol administration in children. *IEEE Transactions on Biomedical Engineering*, bf 60(9), (2013), 2521–2529. DOI: 10.1109/TBME.2013.2259592.

[19] K. Soltesz, G.A. Dumont, K. van Heusden, T. Hagglund, and J.M. Ansermino: Simulated mid-ranging control of propofol and remifentanil using EEG-measured hypnotic depth of anesthesia. *51st IEEE Conference on Decision and Control*, Maui, HI, USA, (2012) 356–361. DOI: 10.1109/CDC.2012.6426858.

[20] Y. Sawaguchi, E. Furutani, G. Shirakami, M. Araki, and K. Fukuda: A model predictive sedation control system under total intravenous anesthesia. *IEEE EMBS Asian-Pacific Conferenc in Biomedical Engineering*, (2003), 358–359. DOI: 10.1109/APBME.2003.1302732.

[21] K. Soltesz; J-O Hahn, G.A. Dumont, and J.M. Ansermino: Individualized PID control of depth of anesthesia based on patient model identification during the induction phase of anesthesia. *50th IEEE Conference on Decision and Control and European Control Conference*, Orlando, FL, USA, (2011). DOI: 10.1109/CDC.2011.6160189.

[22] T.W. Schnider, C.F. Minto, P.L. Gambus, C. Andresen, D.B. Goodale, S.L. Shafer, and E.J. Youngs: The influence of method of administration and covariates on the pharmacokinetics of propofol in adult volunteers. *Anaesthesiology*, **88**(5), (1998), 1170–1182. DOI: 10.1097/00000542-199805000-00006.

[23] K. van Heusden, G.A. Dumont, K. Soltesz, C.L. Petersen, A. Umedlay, N. West, and J.M. Ansermino: Design and clinical evaluation of robust PID control of propofol anaesthesia in children. *IEEE Transactions on Control Systems Technology*, **22**(2), (2014), 491–501. DOI: 10.1109/TCST.2013.2260543.

[24] M. Janda, O. Simanski, J. Bajorat, B. Pohl, G.F.E. Noeldge-Schomburg, and R. Hofmockel: Clinical evaluation of a simultaneous closed-loop anaesthesia control system for depth of anaesthesia and neuromuscular blockade. *Anaesthesia*, **66**(12), (2011), 1112–1120. DOI: 10.1111/j.1365-2044.2011.06875.x.

[25] M. Ilyas, J. Iqbal, S. Ahmad, A.A. Uppal, W.A. Imtiaz and R.A. Riaz: Hypnosis regulation in propofol anaesthesia employing super-twisting sliding mode control to compensate variability dynamics. *IET Systems Biology*, **14**(2), (2020). 59–67. DOI: 10.1049/iet-syb.2018.5080.

[26] J.P. Gauthier, H. Hammouri and S. Othman: A simple observer for nonlinear systems applications to bioreactors. *IEEE Transactions on Automatic Control*, 37(6), (1992), 875–880. DOI: 10.1109/9.256352.

[27] J-J.E. Slotine and W. Li: Applied nonlinear control. Englewood Cliffs, NJ, Prentice Hall, 1991.

[28] A.A.S. Sharif, P.A.H. Badi, S. Mekhilef, and A. Ordys: A new strongly predefined time sliding mode controller for a class of cascade high-order nonlinear systems. *Archives of Control Sciences*, **30**(3), (2020), 599–620. DOI: 10.24425/acs.2020.134679.

[29] T. Yuvapriya, P. Lakshami, and S. Rajendiran: Vibration control and performance analysis of full car active suspension system using fractional order terminal sliding mode controller. *Archives of Control Sciences*, **30**(2), (2020), 295–324. DOI: 10.24425/acs.2020.133501.

[30] P. Akavipat, N. Hungsawanich, and R. Jansin: Alternative placement of bispectral index electrode for monitoring depth of anesthesia during neurosurgery. *Acta Medica Okayama*, **68**(3), (2014), 151–155. DOI: 10.18926/AMO/52655.